Available online at www.sciencedirect.com

SCIENCE DIRECT

Biochimica et Biophysica Acta 1668 (2005) 64–74

BIOCHIMICA ET BIOPHYSICA ACTA
BBA

http://www.elsevier.com/locate/bba

Disturbances of the sarcoplasmic reticulum and transverse tubular system in 24-h electrostimulated fast-twitch skeletal muscle

J.A. Frías[a], J.A. Cadefau[a], C. Prats[a], M. Morán[b], A. Megías[b], R. Cussó[a,*]

[a]*Department of Physiological Sciences I, University of Barcelona, Institut d'Investigacions Biomèdiques August Pi i Sunyer (IDIBAPS), E-08036 Barcelona, Spain*

[b]*Department of Biochemistry and Molecular Biology I, Faculty of Biology, Universidad Complutense, E-28040 Madrid, Spain*

Received 29 January 2004; received in revised form 29 October 2004; accepted 10 November 2004
Available online 28 November 2004

Abstract

Chronic low-frequency stimulation of rabbit tibialis anterior muscle over a 24-h period induces a conspicuous loss of isometric tension that is unrelated to muscle energy metabolism (J.A. Cadefau, J. Parra, R. Cusso, G. Heine, D. Pette, Responses of fatigable and fatigue-resistant fibres of rabbit muscle to low-frequency stimulation, Pflugers Arch. 424 (1993) 529-537). To assess the involvement of sarcoplasmic reticulum and transverse tubular system in this force impairment, we isolated microsomal fractions from stimulated and control (contralateral, unstimulated) muscles on discontinuous sucrose gradients (27–32–34–38–45%, wt/wt). All the fractions were characterized in terms of calcium content, Ca^{2+}/Mg^{2+}-ATPase activity, and radioligand binding of [^{3}H]-PN 200-110 and [^{3}H]ryanodine, specific to dihydropyridine-sensitive calcium channels and ryanodine receptors, respectively. Gradient fractions of muscles stimulated for 24 h underwent acute changes in the pattern of protein bands. First, light fractions from longitudinal sarcoplasmic reticulum, enriched in Ca^{2+}-ATPase activity, R_1 and R_2, were greatly reduced (67% and 51%, respectively); this reduction was reflected in protein yield of crude microsomal fractions prior to gradient loading (25%). Second, heavy fractions from the sarcoplasmic reticulum were modified, and part (52%) of the R_3 fraction was shifted to the R_4 fraction, which appeared as a thick, clotted band. Quantification of [^{3}H]-PN 200-110 and [^{3}H]-ryanodine binding revealed co-migration of terminal cisternae and t-tubules from R_3 to R_4, indicating the presence of triads. This density change may be associated with calcium overload of the sarcoplasmic reticulum, since total calcium rose three- to fourfold in stimulated muscle homogenates. These changes correlate well with ultrastructural damage to longitudinal sarcoplasmic reticulum and swelling of t-tubules revealed by electron microscopy. The ultrastructural changes observed here reflect exercise-induced damage of membrane systems that might severely compromise muscle function. Since this process is reversible, we suggest that it may be part of a physiological response to fatigue.

Keywords: Muscle electrostimulation; Sarcoplasmic reticulum; Triad; Calcium accumulation

1. Introduction

Chronic low-frequency stimulation (CLFS) of fast-twitch muscles has been widely used to study muscle plasticity [1]. During fast-to-slow transformation elicited by CLFS, muscle fibers undergo changes after 24 h that include a marked reduction in isometric tension whilst principal metabolic fuels such as glycogen, glucose, and phosphocreatine are widely recovered. This loss of force has been attributed to the refractoriness of fast glycolytic type IID fibers, without the involvement of energy deficit [2]. This stage shares many characteristics with low-frequency fatigue (LFF), such as low rate of activation, slow recovery, and calcium accumulation [3].

The current hypothesis of muscle activation assumes some mechanical link between the dihydropyridine-sensi-

* Corresponding author. Department of Ciencias Fisiológicas I, Facultad de Medicina, Universidad de Barcelona, C/ Casanova 143, E-08036 Barcelona, Spain. Tel.: +34 934021919; fax: +34 934035882.
E-mail address: mcusso@ub.edu (R. Cussó).

0005-2736/$ - see front matter © 2004 Elsevier B.V. All rights reserved.
doi:10.1016/j.bbamem.2004.11.006

tive voltage sensor (DHPr) from t-tubules (TT) and the calcium channel or "feet" on the surface of the sarcoplasmic reticulum (SR), known as excitation–contraction coupling (ECC) [4]. Altered ECC may impair muscle performance in LFF via reduced calcium release from the SR [5,6].

Calcium entry due to muscle activity is well documented in skeletal muscle [7], and a probable mechanism of Ca^{2+} accumulation has recently been reported to occur in vitro through Na^{+} channels [8]. This calcium rise has also been demonstrated in stimulated fast-twitch muscle, and has been proposed as a possible signal that promotes muscle transformation [9,10]. Recent reports argue that exercise-induced calcium accumulation may cause reduced Ca^{2+} release, and therefore, muscle fatigue [6,11,12]. Although the exact mechanism by which Ca^{2+} alters sarcoplasmic reticulum (SR) function and calcium release remains to be elucidated, calcium-induced activation of proteases and/or phospholipases are clear candidates to be involved in this process [12]. In fact, calcium rise is linked to exercise-induced damage of muscle fibers, a common feature in fatigue models [13]. Muscle damage is also described in CLFS, and includes swelling of the SR [14], vacuolation of the t-system [15], and triad disruption [5]. SR calcium uptake and Ca^{2+}-ATPase activity have been reported to be reduced by different fatigue protocols and CLFS [16]. Current knowledge indicates that reduced Ca^{2+}-ATPase activity is mainly caused by oxidative damage to calcium pump molecules [17,18].

In a previous study, we demonstrated that 24 h of CLFS in rabbit TA elicits long-lasting fatigue at low frequency activation that is unrelated to energy status. Here, we have assessed the relationship between long-term muscle fatigue and alterations in the ultrastructure and function of the SR evoked by increased levels of calcium. To this end, we have characterized membrane disturbances involved in the appearance of muscle fatigue by isolating microsomal fractions from 24-h stimulated TA rabbit muscle and purifying subfractions of SR, T-system, and sarcolemma (SL) on sucrose density gradients. The changes detected in vesicular fractions were confirmed by transmission electron microscopy. We have found that 24 h of CLFS in TA rabbit muscle induced important ultrastructural alterations of the SR as damage to longitudinal SR and swelling of t-tubules that could explain the refractoriness of 24-h stimulated muscles. These changes are reflected on sucrose gradients as a shift in vesicle density possibly associated to the excess of calcium content raised by muscle activity.

2. Materials and methods

2.1. Muscle electrostimulation

Adult female White New Zealand rabbits weighing 2.5–3 kg were pre-anaesthetized by i.m. injection of 1 mg/kg azepromazine maleate (Calmo Neosan, Pfizer) and 0.2 mg/kg atropine sulfate. After 30 min, the animals were anaesthetized by i.m. injection of 50 mg/kg ketamine (Ketolar, Parke-Davis Co.). Electrodes were implanted on both sides of the peroneal nerve of the left hind limb [2]. One week later, the tibialis anterior (TA) muscle was stimulated continuously at 10 Hz (0.15-ms pulse duration, 2–5 V) for 24 h using a telestimulation system [19]. All experiments were approved by the ethics committee of the University of Barcelona and complied with the Guidelines for the Care and Use of Laboratory of Animals (NIH publication, 1985; 86/609/CEE and 214/1997DOG).

2.2. Isolation of microsomal fractions

After 24 h of electrostimulation, the animals were anaesthetized as described above. Next, the stimulated and control (contralateral) TA muscles were quickly removed and then rinsed with ice-cold isolation buffer (5 mM imidazol–HCl pH 7.4, 0.3 M sucrose). The muscles were then processed for separation of microsomal fractions, according to the method of Saito et al. [20] with several modifications (Fig. 1). Basically, individual muscles were cut into small pieces (~5-mm cubes) after separation of connective tissue. The muscle was then homogenized by two 30-s bursts in a Sorval Omnimixer in 5 volumes of isolation buffer supplemented with the following protease inhibitors: 2.5 μg/ml leupeptin, 40 μg/ml PMSF (phenylmethylsulfonyl fluoride), 0.5 μg/ml aprotinin, 0.6 mM benzamide, and 0.5 μg/ml pepstatin. Muscle homogenates (H) were centrifuged at 7700×*g* for 10 min in a Sorval centrifuge at 4 °C. The supernatant (S1) was kept on ice for further fractionation. The pellet (P1) was resuspended in the same volume, rehomogenized as before, and recentrifuged at 7700×*g* to obtain a second supernatant (S2) and pellet (P2). S1 and S2 were filtered through three layers of cheesecloth and used for the sedimentation of microsomal fractions MF1 and MF2, which were representative of different populations of microsomes according to their ease of extraction. Vesicle sedimentation was performed by high-speed centrifugation of S fractions at 110 000×*g* (max.) in a Beckman Ultracentrifuge for 1.5 h. The resulting pellets were carefully collected and homogenized with a glass homogenizer in 0.15 ml of isolation buffer. Aliquots of the different fractions (H, MF1, MF2, and P2) were collected and stored at −80 °C prior to analysis and characterization. All steps were performed at 4 °C.

2.3. Density gradient separation

The crude microsomal fractions MF1 and MF2 were combined in order to improve protein yield and then loaded on a discontinuous sucrose gradient. The gradient consisted of four steps of 2.4 ml (27–32–34–38% sucrose, wt/wt) and one step of 1.4 ml (45% sucrose, wt/wt) sucrose in 5 mM imidazol–HCl pH 7.4. The gradient was used to purify subfractions corresponding to sarcoplasmic

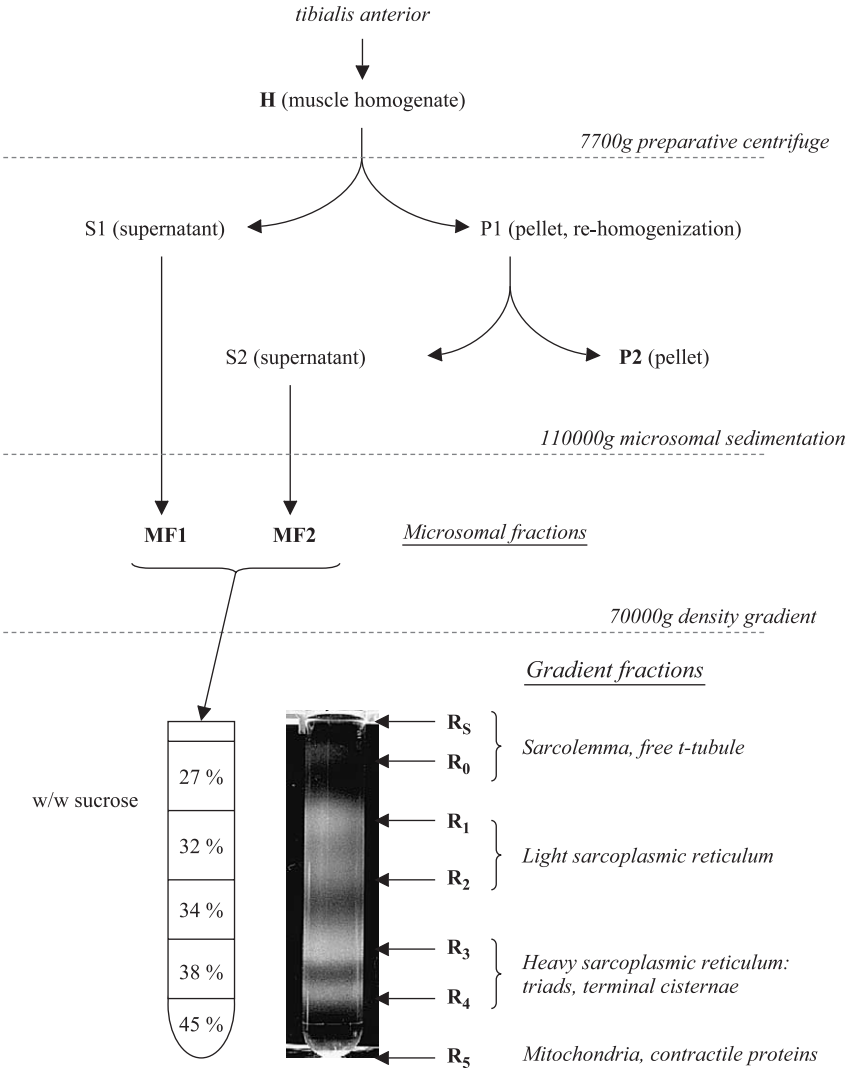

Fig. 1. Diagram of muscle fractionation and isolation of vesicular fractions.

reticulum, t-tubular system, and sarcolemma. Gradients were spun at 70 000×*g* (max.) in a Beckman ultracentrifuge for 12–16 h. Finally, the resulting bands R_S (floating surface material) and R_0–R_5 (from least to most dense, R_5 corresponding to the pellet) were collected and stored at −80 °C (Fig. 1).

2.4. Ca^{2+}/Mg^{2+} -ATPase activity

Enzymatic activity of the SR Ca^{2+}/Mg^{2+}-ATPase was measured using two slightly different spectrophotometric methods, both of them based on enzymatic assay coupled to NADH (nicotinamide adenine dinucleotide) oxidation detected at 340 nm.

Ca^{2+}-ATPase activity was measured in muscle homogenates (H) and pellets of the 2nd homogenization (P2) at 37 °C, according to Saborido et al. [21]. Briefly, the standard reaction mixture contained 25 mM MOPS (3-(*N*-morpholino) propanesulfonic acid), 1 mM EGTA (ethylene glycol bis [β-aminoethyl ether]-N,N,N',N'-tetraacetic acid), 15 mM $MgCl_2$, 200 mM KCl, 10 mM phosphoenolpyruvate, 2.4 U/ml pyruvate kinase, 10 U/ml lactate dehydrogenase, and 0.27 mM NADH in a final volume of 1 ml. SR Ca^{2+}-ATPase activity was measured by means of two parallel assays, using a high (21 mM) Ca^{2+} concentration to selectively inhibit SR Ca^{2+}-ATPase activity [22]. The standard assay medium at pH 7.0 also contained 1 or 21 mM $CaCl_2$, 10 mM sodium azide, 0.005% Triton X-100, and an appropriate amount of protein (0.1 mg wet tissue weight). The reaction was initiated by the addition of 4 mM ATP. The rate of ATP hydrolysis was calculated from the NADH oxidation measured at 340 nm (ε=6.22 $mM^{-1} \cdot cm^{-1}$). The difference between the rates measured with 1 mM $CaCl_2$ (total ATPase activity: Ca^{2+}-ATPase+background ATPase activity) and 21 mM $CaCl_2$ (background ATPase activity) represents the SR Ca^{2+}-ATPase activity.

Crude microsomal fractions and gradient subfractions were assayed according to Saborido et al. [23] with several modifications. Mg^{2+}-dependent ATPase activity was meas-

ured at 30 °C in a reaction mixture containing 25 mM MOPS pH 7.4, 0.2 mM EGTA, 5 mM $MgCl_2$, 100 mM KCl, 5 mM sodium azide, 0.6 mM phosphoenolpyruvate, 0.28 mg/ml NADH, 10 U/ml pyruvate kinase, 2 U/ml lactate dehydrogenase, and 5–10 μg of microsomal protein. The reaction was initiated by addition of 1 mM ATP. Ca^{2+}-ATPase activity was determined as the difference between basal Mg^{2+}-dependent activity and the total activity in the presence of 0.2 mM Ca^{2+} and 0.2 μg/ml of the calcium ionophore A23187 (Sigma, USA).

2.5. [^{3}H]-PN 200-110 and [^{3}H]-ryanodine binding assays

Dihydropyridine-sensitive calcium channels from t-tubules (DHPr) were quantified according to Delgado et al. [24]. Binding of (+)-[^{3}H]-PN200-110 (70 Ci/mmol; DuPont-New England Nuclear) was performed in triplicate with 3 nM [^{3}H]-PN200-110 in a 1-ml reaction mixture containing 50 mM Tris–HCl pH 7.4, 1 mM $CaCl_2$, 1 mM $MgCl_2$, and the appropriate amount of protein (~5–10 μg of protein for microsomal fractions and ~30–50 μg for gradient fractions). Incubations were carried out in the dark for 2 h at 25 °C. Nonspecific binding was determined in the presence of 1 μM unlabelled nitrendipine (Bayer). Incubations were stopped by rapid filtration of samples through Whatman GF/B filters soaked in ice-cold buffer (50 mM Tris–HCl, pH 7.4) under reduced pressure. The filters were washed five times with 4-ml ice-cold buffer and the radioactivity remaining on the filters was determined by liquid scintillation counting with Ecoscint H scintillation cocktail (National Diagnostics, USA).

Ryanodine-sensitive calcium channels from the SR (RyR) were quantified by specific binding of [^{3}H]ryanodine (68 Ci/mmol; DuPont-New England Nuclear), according to the method of Sapp and Howlett [25]. Aliquots of the preparations (~10 μg of protein for microsomal fractions and ~50 μg for gradient fractions) were incubated in triplicate with 10 nM [^{3}H]-ryanodine in 1 ml of buffer containing 50 mM MOPS pH 7.4, 1 M KCl, 0.1 mM EGTA, and 0.2 mM $CaCl_2$. Binding was carried out at 25 °C for 2 h. Nonspecific binding was determined in the presence of 10 μM unlabelled ryanodine. After incubation, filters were washed five times with 4-ml ice-cold buffer (50 mM MOPS pH 7.4, 1 M KCl) and radioactivity was quantified as above.

2.6. Total calcium

Total calcium was measured by atomic absorption in a flame spectrophotometer (Perkin Elmer) using LaCl as phosphate chelator. Calcium was released from samples (10–100 μg of protein) by dilution (1:1) in 0.6 M trichloracetic acid, reaching a final concentration of 0.3 M. Then, samples were spun in a microfuge, and the resulting supernatant was removed for calcium determination.

2.7. Electron microscopy

Tissue samples were processed as described previously [26]. Small pieces (0.2–0.5 mm. cubes) from 24-h stimulated and contralateral muscles were quickly excised and fixed at 4 °C in 100 mM sodium cacodylate pH 7.2–7.3 containing 8% (w/v) sucrose, 1% (w/v) tannic acid, and 2% (v/v) glutaraldehyde.

Vesicles from gradient fractions control R_3 and R_4, and R_4 from stimulated muscles were fixed in suspension, directly in the gradient medium. Samples were slowly (~15 s) mixed with 0.1 volume of 25% (v/v) glutaraldehyde, 200 mM sodium cacodylate pH 7.2, at 4 °C [27].

Postfixation was carried out in 1% OsO_4 and 0.8% $K_3Fe(CN)_6$ (w/v) at 4 °C for 2 h in muscle tissue and overnight in vesicle preparations. Then, samples were dehydrated in acetone followed by embedding in Spurr.

2.8. Statistical analysis

All assays were performed at least in duplicate. Means±S.E. of three to five independent preparations are presented. Effects of 24-h stimulation on the variables studied were analysed statistically using the Student's *t* test. Results were considered statistically significant when $P<0.05$.

3. Results

3.1. Characterization of microsomal fractions

MF1 and MF2, which were relatively crude preparations, were characterized using various markers (Table 1). The MF1 fraction is thought to be composed of heterogeneous material: SL, free TT, and a high proportion of light SR, which is easily released during the first burst of homogenization, as indicated by its higher Ca^{2+}-ATPase activity and lower [^{3}H]-ryanodine and [^{3}H]-PN 200-110 binding. In contrast, MF2, as shown by its higher [^{3}H]-ryanodine and [^{3}H]-PN 200-110 binding and lower Ca^{2+}-ATPase activity, is enriched in heavy fractions of SR, such as TC and triads, which are more difficult to extract from the tissue. However, MF2 had similar values of Ca^{2+}-ATPase activity to MF1 (Table 1).

CLFS induced changes in microsomal fractions. First, the protein yield of the MF1 fraction was significantly reduced in stimulated muscle (~25%). This suggests a selective loss of light vesicles of SR during isolation, or selected proteolysis of longitudinal SR proteins, given that the total number of DHPr and RyR (triads, terminal cisternae) remained constant (Table 1). Second, electrical stimulation significantly reduced calcium pump activity in the MF1 fraction, suggesting that only selected parts of the SR are affected by the electrical stimulation protocol. Moreover, basal Ca^{2+}-ATPase activity rose significantly in both MF1

Table 1
Characterization of muscle homogenates and microsomal fractions

Fraction	H		P2		MF1		MF2	
	Control	24-h stimulated	Control	24-h stimulated	Control	24-h stimulated	Control	24-h stimulated
Protein yield	23.6±2.1	23.6±1.7	10.0±0.5	10.9±0.2	3.4±0.5	2.3±0.5*	2.3±0.2	2.0±0.2
Ca^{2+}-ATPase	81.7±6.6	76.8±8.2	31.8±3.5	38.0±2.7	3.1±0.1	1.9±0.2*	2.0±0.3†	1.3±0.1
Mg^{2+}-ATPase	–	–	–	–	0.38±0.01	0.47±0.01*	0.18±0.01†	0.25±0.01*,†
DHPr	–	–	–	–	1.1±0.2	1.3±0.1	4.7±0.3†	4.4±0.2†
RyR	–	–	–	–	1.9±0.3	1.9±0.2	3.4±0.7	2.9±0.4

Protein yields of H (muscle homogenates) and P2 (pellet of second homogenization) are expressed as mg/ml. Protein yields of MF1 and MF2 are expressed as mg of total protein. Ca^{2+}-ATPase activity and its corresponding basal activity (Mg^{2+}-dependent) are expressed as μmol ATP mg^{-1} min/g (units/g fresh tissue) at 30 °C. Ca^{2+}-ATPase activity of muscle homogenates and pellet P2 measured at 37 °C according to Saborido et al. [26]. Data are expressed as U/g fresh tissue. Quantification of DHPr is expressed as pmol [^{3}H]-PN 200-110/g fresh tissue. Quantification of RyR is expressed as pmol [^{3}H]-ryanodine/g fresh tissue.

* Significantly different from control.

† Significantly different from MF1. Data are expressed as mean±S.E. $P<0,01$, $n=3–5$.

and MF2. This activity is mainly linked to a t-tubular ectoenzyme, the Mg^{2+}-ATPase [23]. These observations can be explained by a selective loss of light SR vesicles, increasing the specific activity of the t-tubular Mg^{2+}-ATPase.

In parallel, muscle homogenates (H) and pellet P2 (remaining cellular material) were assessed for total SR Ca^{2+} pump activity using a second method suitable for total homogenates [22]. This allowed the reduction in Ca^{2+}-ATPase activity detected in microsomal fractions to be confirmed. Surprisingly, total SR Ca^{2+}-ATPase activity did not change significantly in H and P2. The maintenance of Ca^{2+}-ATPase activity in muscle homogenates implies that the reduction detected in MF1 is mainly due to effects other than a reduction in the specific activity of the enzyme.

Analysis of nitrendipine and ryanodine binding to the vesicular fractions provides information about the number of dyhidropyridine and ryanodine-sensitive calcium channels, and the type of vesicles (TT or SR in origin). MF1/MF2 did not show differences in either total [^{3}H]-PN 200-110 or [^{3}H]-ryanodine binding between stimulated and contralateral muscle (Table 1). Therefore, as indicated above, the reduction in protein yield is restricted to light SR, as quantification of RyR and DHPr from TC and TT remained constant.

3.2. Density gradient fractions

Fractionation of a mixture of MF1 and MF2 was performed on discontinuous sucrose gradients in order to separate SL, TT, and SR membranes. Isopycnic gradients from control muscle contained a floating band, five layers of different density, and a pellet (Fig. 1). These layers of R_S and R_0–R_5 material (see Materials and methods) were characterized by analysis of Ca^{2+}/Mg^{2+}-ATPase activity and [^{3}H]-PN 200-110 and [^{3}H]-ryanodine binding (Table 2a). From these results, and given the floating density of the different layers recovered, we classified R_S and R_0 as SL and free TT vesicles, respectively, because of their high basal Mg^{2+}-dependent activity. R_1 and R_2 were classified as light SR on the basis of their high levels of calcium pump activity. R_3-R_4 corresponded to heavy SR (triads and TC), as indicated by their high levels of [^{3}H]-PN 200-110 and [^{3}H]-ryanodine binding. Finally, R_5 did not give a clear positive result in any of the assays performed, and probably corresponds to heavy material such as mitochondria and contractile proteins [20]. These gradient fractions from contralateral muscle (Table 2) were consistent with the bands described by Saito [20]. The 34–38% and 38–45% interphase bands, described by Saito as triads/TC and isolated TC vesicles, corresponded to heavy fractions of SR in our preparations, exhibiting high [^{3}H]-PN 200-110 and [^{3}H]-ryanodine binding and DHPr/RyR ratios of ~1 (R_3) and ~0.5 (R_4). Neither R_3 nor R_4 met the DHPr-to-RyR ratio of 2 described previously in rabbit muscle triads [28], although an overall ratio of ~1 in fast-twitch rabbit muscle has previously been described [29]. In control gradients, the inclusion of microsomes from the first homogenization, which was discarded in the original protocol described by

Table 2
Characterization of gradient fractions from control and 24-h stimulated muscles

Fraction	Mg^{2+}-dependent	Ca^{2+}-ATPase	DHPr	RyR
(a) Control				
R_S	0.23±0.03	–	0.28±0.18	–
R_0	0.58±0.26	0.36±0.16	2.46±1.44	0.70±0.83
R_1	0.29±0.01	5.93±0.42	1.45±0.22	0.50±0.06
R_2	0.19±0.01	5.71±1.02	1.26±0.19	0.58±0.35
R_3	0.24±0.01	4.18±0.89	5.66±0.98	5.86±0.87
R_4	0.16±0.02	2.52±0.70	2.77±0.57	6.82±1.62
R_5	0.13±0.01	1.03±0.18	0.60±0.12	1.29±0.39
(b) 24-h stimulated				
R_S	0.26±0.01	–	0.43±0.42	0.71±0.63
R_0	0.92±0.17	0.18±0.03	1.66±0.34	0.04±0.02
R_1	0.99±0.18*	3.21±0.31*	2.70±0.45	0.25±0.06*
R_2	0.41±0.13	3.25±0.51	1.96±0.59	0.54±0.12
R_3	0.30±0.03	2.83±0.15	3.39±0.34	4.04±0.78
R_4	0.27±0.07	1.94±0.58	5.00±0.14*	6.16±0.30
R_5	0.19±0.04	1.26±0.06	0.59±0.28	2.38±0.34

Basal Mg^{2+}-dependent activity and Ca^{2+}-ATPase activity were determined at 30 °C. Both activities are expressed as U/mg protein. (RyR) Ryanodine-sensitive calcium channels are expressed as pmol [^{3}H]-ryanodine/mg protein. (DHPr) Dihydropyridine-sensitive calcium channels are expressed as pmol [^{3}H]-PN 200-110/mg protein. Data are expressed as mean±S.E.

*$P < 0.05$, $n=3–5$.

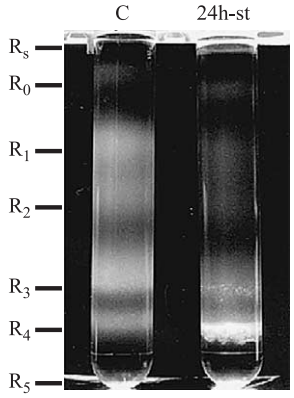

Fig. 2. Sucrose density gradient from control and 24-h stimulated muscle. Sucrose density gradients from control (C) and 24-h stimulated muscles (24h-st). The fractions collected as R_S and $R_{0–5}$ are indicated in the left-hand margin.

Saito, resulted in an enrichment of the R_1 and R_2 fractions in high Ca^{2+}-dependent ATPase activity vesicles of light SR origin. However, R_S and R_0, described by Saito as SL or TT-free elements, showed very low values for all parameters measured and had a low protein yield. This indicates that most TT elements were attached to TC vesicles, as would be expected in a high-density medium with low ionic strength.

As shown in Fig. 2, we found two dramatic changes in the appearance and thickness of the different layers in gradients from 24-h stimulated muscles. Layers R_1 and R_2 (light SR), and R_3 (heavy SR) were reduced in size by 67%, 51%, and 52%, respectively. R_4 was thicker, and had clotted appearance. [^{3}H]-PN 200-110 and [^{3}H]-ryanodine binding in gradient bands (Fig. 3, Table 2) revealed a dramatic shift in the buoyant density of vesicles from the R_3 band now being recovered in the R_4 fraction in 24-h stimulated muscles. The elements in R_3, of TC and TT origin, shift

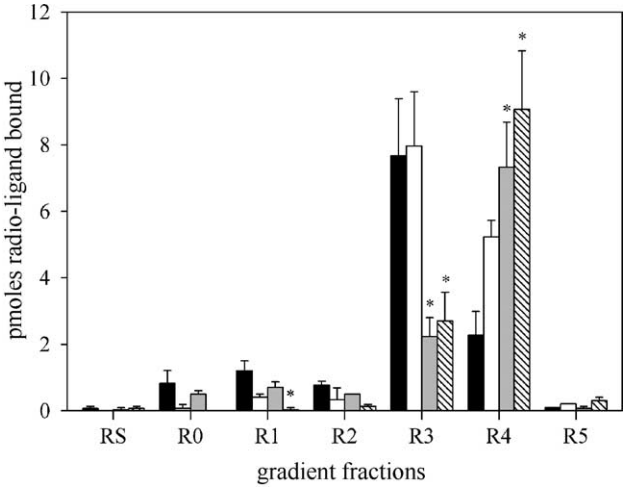

Fig. 3. Quantification of calcium channels in the sucrose gradient fractions. Dihydropyridine-sensitive calcium channel from t-tubules of control (■) and 24-h stimulated (▩) muscles, and ryanodine-sensitive calcium channel from terminal cisternae of control (□) and 24-h stimulated (▨) muscles. Units are picomoles of bound [^{3}H]-PN 200-110 or [^{3}H]ryanodine. Data are expressed as mean±S.E. (n=3–5, P<0.01).

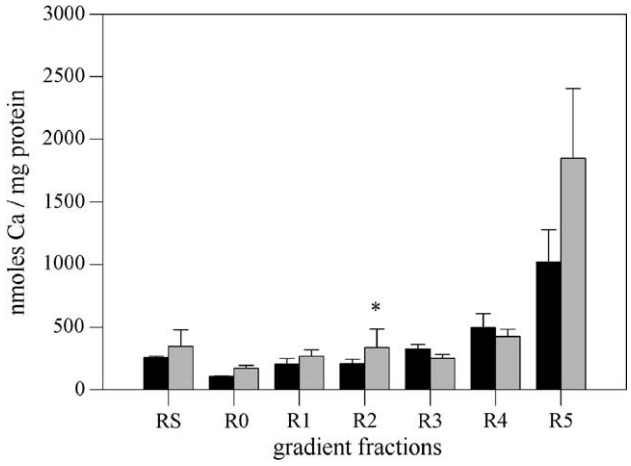

Fig. 4. Total calcium content in gradient fractions: (■) control muscle; (▩) 24-h stimulated muscle. Data are expressed as mean±S.E. (n=3–5, *P<0.01).

their position from R_3 to R_4 in 24-h stimulated muscles, as demonstrated by the maintenance of the DHPr-to-RyR ratio in R_3 (Table 2). This is consistent with the presence of triads in the R_3 fraction. The changes in density after 24 h of muscle stimulation were reversed after 24–48 h of rest. These alterations are long-lasting, in line with the depression of force in fatigued skeletal muscle (data not shown).

3.3. Calcium content

We assessed the possibility that the density change in vesicles could be related to exercise-induced calcium accumulation inside the SR. Although we detected no significant increments of calcium content in any gradient fractions, except for a small rise in R_2 and a nonsignificant rise in R_5 (Fig. 4), an involvement of calcium accumulation cannot be discounted. In fact, R_3 vesicles could achieve the same calcium level as R_4, increasing their

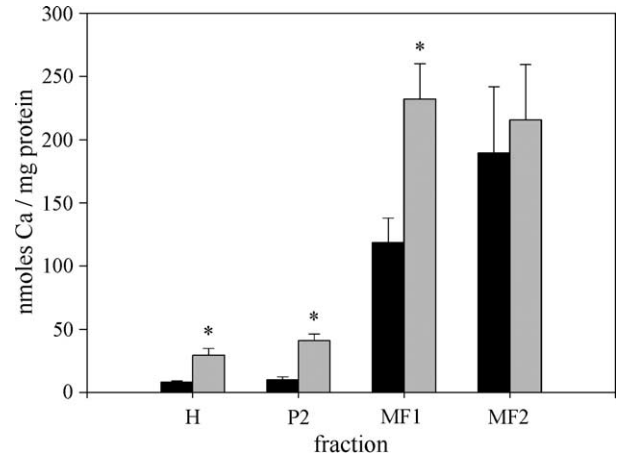

Fig. 5. Calcium content in the cellular fractions. (H) homogenate; (P) pellet of 7700×g; (MF1 and MF2) microsomal fractions of 110 000×g pellets. (■) Control muscle; (▩) 24-h stimulated muscle. Data (nmol mg^{-1} of protein) are expressed as the mean±S.E. (n=3–5, *P<0.01).

density without any increase in calcium content per milligram of protein.

Electrical stimulation of rat TA and EDL muscles leads to a marked accumulation of total calcium [7]. Therefore, we hypothesized that calcium accumulation in SR or other cellular organelles is involved in the alterations observed in sucrose gradients from stimulated muscles. As shown in Fig. 5, total calcium content is three to four times greater in 24-h stimulated muscle homogenates (H). This increase is maintained in the P2 fraction, demonstrating that either the large calcium overload is not stored in SR or that homogenization of muscle causes leakage of calcium from the SR and its binding to sedimented proteins in pellet P2. In contrast, only MF1 of stimulated muscles showed a significant rise in calcium content.

3.4. Transmission electron microscopy

Electron microscopy revealed marked differences in the ultrastructure of contralateral and stimulated muscles. Contralateral muscle displayed regular placing of sarcomeres with alignment of Z-lines and preserved ultrastructure of the SR, in which triads were correctly placed at the level of A and I bands (Fig. 6a). In these muscles, TC are well-shaped, contain electron-dense material, and are attached to their corresponding TT. Light SR, although not fully visible, also appears to be preserved. Fig. 6b shows the control SR with the triads and TT at higher magnification.

Fig. 6c shows the 24-h stimulated muscle. Electrical stimulation induced a number of disturbances in muscle ultrastructure. Sarcomeres were irregularly placed, and

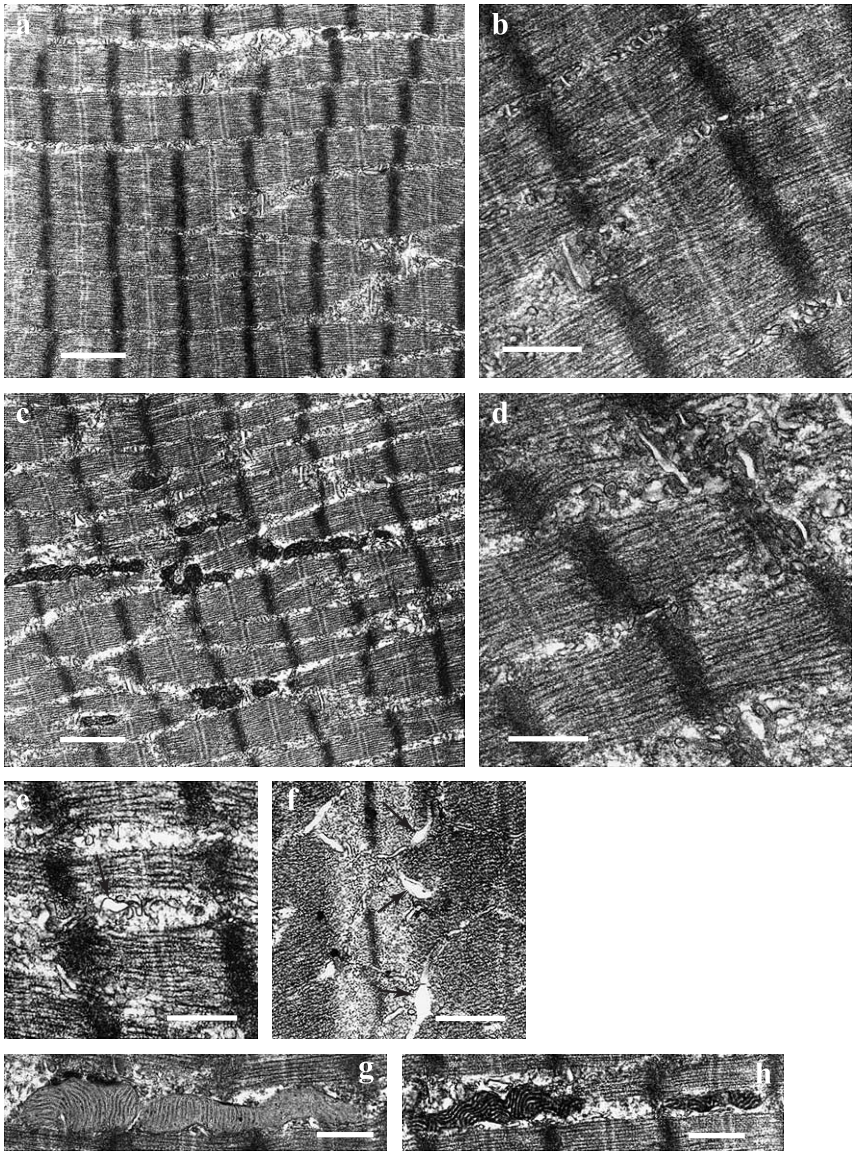

Fig. 6. Transmission electron microscopy of rabbit TA muscle. (a) Control muscle. (b) Control muscle at higher magnification. (c) 24-h stimulated muscle. (d) 24-h stimulated muscle at higher magnification. (e and f) Detail of swollen areas in t-tubules (arrows) in 24-h stimulated muscle. (g) Mitochondria from control muscle. (h) Mitochondria from 24-h stimulated muscle. Scale bars in a and c represent 2 μm. Scale bars in b, d, e, f, g, and h represent 1 μm.

myofibrils disrupted in many places. The SR structure was severely damaged, and longitudinal SR was either disintegrated or distorted and swollen in some areas. Fig. 6d shows a higher magnification view of distorted areas of the SR in 24-h stimulated muscle, swollen areas being mainly restricted to TT (Fig. 6e and f). The myofilaments of stimulated muscle were thicker and irregularly aligned in sarcomeres. This hyperplasia is probably related to edema, common in stimulated muscles.

Mitochondria were severely affected by electrical stimulation, becoming smaller and much more electron dense. They were frequently located in distorted areas around the SR, some of them close to t-tubules or coiled around the SR (Fig. 6c). Crests were wider and distorted, mainly oriented longitudinally (Fig. 6h), whereas control organelles exhibited a normal matrix with a smoother transversal crest (Fig 6g).

Electron-microscopic observation of fractions from the sucrose gradient (Fig. 7a) shows that fraction R_3 from control muscles contains two types of vesicles. The first type corresponds to TC, which are spherical vesicles with electron-dense material inside corresponding to the Ca^{2+}-binding protein calsequestrin (CS). Some of these vesicles show the connection between internal CS and the junctional face of the TC at which RyR-sensitive Ca^{2+} channels are located. In fact, the presence of triads could also be detected. Other types of vesicles are elongated and flat, some of them appearing attached to the TC, revealing them to be TT. Vesicles from fraction R_4 of control muscle (Fig. 7b) are of the same type as found in R_3, although here TC appear more frequently than in R_3.

The shape and size of vesicles detected in stimulated R_4 were different from those found in controls (Fig. 7c1). TC vesicles were less predominant, and their shape was altered. Large vesicles appeared, some of which contained small vesicles resembling fragments of mitochondria. Other vesicles were coiled (Fig. 7c2). Furthermore, many small particles were diffusely distributed around vesicles like "dust". In some areas, vesicles and particles seemed to be joined or grouped.

4. Discussion

In this study, we have presented biochemical and ultrastructural evidence that 24 h of CLFS in rabbit TA muscle promotes alterations affecting two different membrane systems: first, damage to longitudinal SR, and second, the alteration of triadic structure, such as swelling of t-tubules. To study these alterations in the sarcotubular system, we adapted the isolation method for TC vesicles described by Saito et al. [20]. This method allows vesicles to be obtained that are representative of all membrane systems, and preserves membrane structure by virtue of the fact that it does not include the salt treatment usually employed to remove contractile proteins. The preservation of membrane

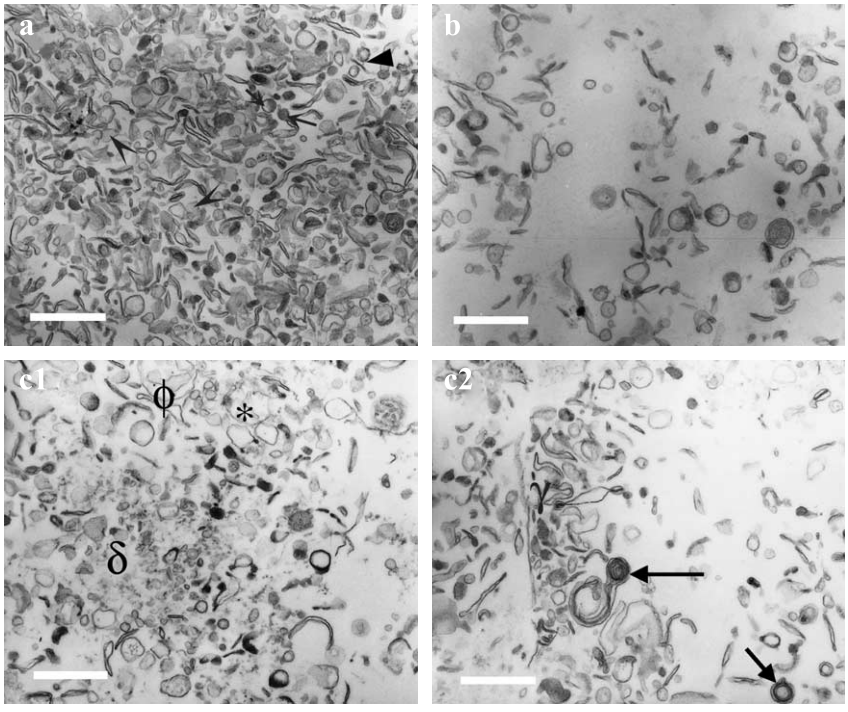

Fig. 7. Transmission electron microscopy of isolated sarcoplasmic reticulum. (a) Vesicles from R_3 fraction (34–38% interphase) of control muscle; TC vesicles with electron-dense material inside (arrows); Triads (solid arrowheads); t-tubules (open arrowheads). Scale bars represent 1 μm. (b) Vesicles from the R_4 fraction (38–45% interphase) of control muscle. (c1 and c2) Vesicles from the R_4 fraction of 24-h stimulated muscle. Large vesicles with irregular shape (*); coiled vesicles (arrows, solid head); vesicles containing smaller vesicles (ϕ); small vesicles appearing as 'dust' (δ); grouped vesicles and particles (γ). Scale bars represent 1 μm.

structure was crucial to the maintenance of vesicle integrity and the preservation of interactions (e.g., at the triadic junction), and furthermore, allowed processing for electron microscopy studies [26].

The most abundant protein in the longitudinal SR is the calcium pump. This Ca^{2+}-ATPase activity did not change in muscle homogenates after stimulation, although a significant reduction of MF1, R_1 and R_2 bands was detected in gradients from stimulated muscles. This loss of activity in some fractions could be linked to the significant reduction in the protein yield of MF1 and MF2. Thus, stimulation promotes ultrastructural alterations of light SR, which in turn alters the behaviour of vesicles during isolation and causes a lack of recovery from microsomal fractions. We detected a significant enrichment in Mg^{2+}-dependent ATPase activity in microsomal and gradient fractions. This Mg^{2+}-ATPase is known to be located in TT membranes as an ectoenzyme [23], indicating that the loss of protein in microsomal fractions selectively enriches TT vesicles [30]. Electron microscopy images show a marked distortion and disruption of longitudinal SR, which could induce the formation of damaged vesicles, such as smaller or unsealed vesicles, during homogenization. SR damage could be caused by membrane degradation via phospholipase activation [14] or peroxidation by free radicals.

Calcium overload causes phosphate-induced precipitation inside the SR of exercised muscles [31,32]. This could make vesicles heavier; in which case, these longitudinal SR vesicles would be more dense, and would modify their behaviour in the sucrose gradient.

In a similar model, Matsushita et al. [33] demonstrated reductions in Ca^{2+}-ATPase activity and Ca^{2+} transport in short-term electrostimulated rabbit muscle that were related to alterations in the ATP-binding domain of the enzyme [16], and restricted to a specific SR vesicle population. Although our stimulation protocol differs from that used by Matsushita and co-workers, we also detected an ~30–40% reduction in Ca^{2+}-ATPase activity, only in the vesicles from MF1, specially enriched in light SR. As mentioned above, we attribute this ATPase reduction to a selective loss of longitudinal SR vesicles. Other authors have suggested that proteolysis of damaged Ca^{2+}-ATPase molecules after short-term electrostimulation in rat skeletal muscle is responsible for the decreased activity [17]. In this respect, only a small rise in m-calpain and its translocation to the membrane fraction was detected in our laboratory in the same model at this period [34].

The most significant changes in gradients from 24-h stimulated muscles were confined to heavy fractions of the SR, R_3 being significantly reduced in size and R_4 appearing as a thick, clotted band with a large accumulation of vesicles. As shown by the results of [^{3}H]-PN 200-110 and [^{3}H]-ryanodine binding (Table 2a–b, Fig. 3), there is no doubt that R_3 vesicles underwent a change in density, shifting to the R_4 fraction. The reduction in [^{3}H]-PN 200-110 and [^{3}H]-ryanodine binding occurred to similar degrees in the R_3 fraction, demonstrating co-migration of TT and TC elements, which suggests the presence of junctional vesicles as triads or dyads in R_3. Several authors have argued that increased inorganic phosphate levels during fatigue may induce calcium precipitation inside the SR, thereby reducing calcium release [35]. To explore the involvement of calcium accumulation in this density change, we measured total calcium content in homogenate, P2, and gradient fractions. The increase in Ca^{2+} concentration seen in the total homogenates suggests that an influx of exogenous Ca^{2+} occurred, and that although this Ca^{2+} was shared by all fractions, its accumulation was particularly notable in the MF1 fraction, probably in the light SR. Otherwise in gradient fractions, this accumulation of exogenous Ca^{2+} in SR could only be proven in the R_2 fraction (corresponding to light SR) but not in the R4 fraction. It is possible that vesicles from R_3 have the same calcium level as those of R_4, and that they shifted to R_4. The calcium content in pellet P2 in stimulated muscle shows a similar three- to fourfold increase as seen in total homogenates. This fraction is expected to be composed of a mixture of heavy elements, such as nuclei, contractile proteins, and indeed, mitochondria. Therefore, it seems plausible that mitochondria could play an important role in the buffering of calcium overload. Electron microscopy of muscle supports the hypothesis of mitochondrial alterations, exhibiting altered morphology, electron-dense matrix, and irregular crestae.

Several reports have proposed the existence of vesicular alterations in TC or TT in fatigued or stimulated skeletal muscle. Lannergren et al. [15] described the appearance in *Xenopus* of large vacuoles of unknown origin in fatigued skeletal muscle fibers in communication with TT. Lamb et al. describe the effects of Ca^{2+} rise on the structure of triads, which are distorted or broken in skeletal muscle fibers from rat and toad. These authors suggested a link between the ultrastructural alterations and the uncoupling of the excitation–contraction process [5].

The results shown here from transmission electron microscopy provide new insights into the precise ultrastructural alterations of the SR. Electrical stimulation induced disruption of myofilaments and severe damage to SR ultrastructure. The longitudinal SR became disintegrated and distorted; swollen areas were mainly restricted to t-tubules. Due to the junctional link between TT and TC vesicles, changes in any of the components of the triads also affect the linked vesicles. Therefore, this TT swelling could be responsible for the increase in buoyant density of triads detected in the gradients of stimulated muscles. The buoyant density of vesicles depends on both their lipid-to-protein ratio and their content. As TT vesicles have a lower lipid-to-protein ratio than TC, the content of TT vesicles should be dependent upon this density change. Ionic alterations in stimulated muscles, such as Na^+ entry coupled with K^+ exit or Ca^{2+} accumulation, could be involved in osmotic imbalance, producing swelling of TT. Also, the involvement of the T system as a way of eliminating excess calcium

could cause an increase in the density of TT vesicles during isolation, and account for the fraction shift observed in sucrose gradients. In fact, as intracellular calcium accumulation reaches its maximum after 6 h of CLFS (data not shown), at 24 h muscle fibers eliminate the calcium overload. In this process, TT is the route through which calcium and/or damaged structures are eliminated.

In conclusion, CLFS induces calcium entry into muscle fibers. This Ca^{2+} rise is initially buffered by the SR and mitochondria, but it could activate calcium-dependent proteases and phospholipases affecting membrane integrity of the SR, both in longitudinal SR and in triadic structure. This disturbs the excitation–contraction coupling mechanism and so impairs force production conducting the fast-twitch fibers to a refractorious state. This strategy protects the fast-twitch fiber from an energy deficit by allowing the fiber to rest and restore its energetic store, avoiding more deleterious effects of a permanent Ca^{2+} rise. If stimulation stops, all these changes are reversible and may be part of the physiological response to long -term fatigue. If CLFS continues, the loss of part of the SR is characteristic of fast- to slow-twitch fiber transformation. The most interesting observation in our work is that ionic perturbance produces early modification in the SR structure responsible for the temporary refractoriness to stimulation that allows to restore the force generation with rest or to engage the fiber in the transformation process.

Acknowledgements

We would like to thank Nuria Cortadellas and the Serveis Cientifico-Tecnics of the University of Barcelona for sample preparation for electron microscopy. We are also grateful to Professor Alfonso Blanco of the University of Cordoba (Spain) for essential scientific advice on the ultrastructure of skeletal muscle. We are grateful to Mr. Robin Rycroft for editorial support.

C. Prats and J.A. Frías are supported by IDIBAPS postgraduate fellowships. J.A. Cadefau is the recipient of a Spanish Ministry of Science and Technology postdoctoral fellowship. This work was supported by grants PM97-0015 and BFI2001-2944 from the Spanish Ministry of Science and Technology, and by FIS of the Instituto de Salud Carlos III (Red de Centro RCMN-C03/08), Spain.

References

[1] D. Pette, G. Vrbova, Adaptation of mammalian skeletal muscle fibers to chronic electrical stimulation, Rev. Physiol., Biochem. Pharmacol. 120 (1992) 115–202.
[2] J.A. Cadefau, J. Parra, R. Cusso, G. Heine, D. Pette, Responses of fatigable and fatigue-resistant fibres of rabbit muscle to low-frequency stimulation, Pflugers Arch. 424 (1993) 529–537.
[3] D.A. Jones, High- and low-frequency fatigue revisited, Acta Physiol. Scand. 156 (1996) 265–270.
[4] G. Meissner, X. Lu, Dihydropyridine receptor–ryanodine receptor interactions in skeletal muscle excitation–contraction coupling, Biosci. Rep. 15 (1995) 399–408.
[5] G.D. Lamb, P.R. Junankar, D.G. Stephenson, Raised intracellular [Ca^{2+}] abolishes excitation–contraction coupling in skeletal muscle fibres of rat and toad, J. Physiol. 489 (Pt. 2) (1995) 349–362.
[6] H. Westerblad, S. Duty, D.G. Allen, Intracellular calcium concentration during low-frequency fatigue in isolated single fibers of mouse skeletal muscle, J. Appl. Physiol. 75 (1993) 382–388.
[7] M.E. Everts, T. Lomo, T. Clausen, Changes in K^+, Na^+ and calcium contents during in vivo stimulation of rat skeletal muscle, Acta Physiol. Scand. 147 (1993) 357–368.
[8] H. Gissel, T. Clausen, Excitation-induced Ca^{2+} uptake in rat skeletal muscle, Am. J. Physiol. 276 (1999) R331–R339.
[9] F.A. Sreter, J.R. Lopez, L. Alamo, K. Mabuchi, J. Gergely, Changes in intracellular ionized Ca concentration associated with muscle fiber type transformation, Am. J. Physiol. 253 (1987) C296–C300.
[10] J.D. Bruton, J. Lannergren, H. Westerblad, Mechanisms underlying the slow recovery of force after fatigue: importance of intracellular calcium, Acta Physiol. Scand. 162 (1998) 285–293.
[11] E.R. Chin, D.G. Allen, The role of elevations in intracellular [Ca^{2+}] in the development of low frequency fatigue in mouse single muscle fibres, J. Physiol. 491 (Pt. 3) (1996) 813–824.
[12] H. Westerblad, J.D. Bruton, D.G. Allen, J. Lannergren, Functional significance of Ca^{2+} in long-lasting fatigue of skeletal muscle, Eur. J. Appl. Physiol. 83 (2000) 166–174.
[13] H. Gissel, T. Clausen, Excitation-induced Ca^{2+} influx and skeletal muscle cell damage, Acta Physiol. Scand. 171 (2001) 327–334.
[14] S.K. Byrd, Alterations in the sarcoplasmic reticulum: a possible link to exercise-induced muscle damage, Med. Sci. Sports Exerc. 24 (1992) 531–536.
[15] J. Lannergren, J.D. Bruton, H. Westerblad, Vacuole formation in fatigued single muscle fibres from frog and mouse, J. Muscle Res. Cell Motil. 20 (1999) 19–32.
[16] S. Matsushita, D. Pette, Inactivation of sarcoplasmic-reticulum Ca(2+)-ATPase in low-frequency-stimulated muscle results from a modification of the active site, Biochem. J. 285 (Pt. 1) (1992) 303–309.
[17] S. Matsunaga, S. Harmon, B. Gohlsch, K. Ohlendieck, D. Pette, Inactivation of sarcoplasmic reticulum Ca(2+)-ATPase in low-frequency stimulated rat muscle, J. Muscle Res. Cell Motil. 22 (2001) 685–691.
[18] B.M. Klebl, A.T. Ayoub, D. Pette, Protein oxidation, tyrosine nitration, and inactivation of sarcoplasmic reticulum Ca^{2+}-ATPase in low-frequency stimulated rabbit muscle, FEBS Lett. 422 (1998) 381–384.
[19] G. Schwarz, E. Leisner, D. Pette, Two telestimulation systems for chronic indirect muscle stimulation in caged rabbits and mice, Pflugers Arch. 398 (1983) 130–133.
[20] A. Saito, S. Seiler, A. Chu, S. Fleischer, Preparation and morphology of sarcoplasmic reticulum terminal cisternae from rabbit skeletal muscle, J. Cell Biol. 99 (1984) 875–885.
[21] A. Saborido, J. Delgado, A. Megias, Measurement of sarcoplasmic reticulum Ca^{2+}-ATPase activity and E-type Mg^{2+}-ATPase activity in rat heart homogenates, Anal. Biochem. 268 (1999) 79–88.
[22] W.S. Simonides, C. van Hardeveld, An assay for sarcoplasmic reticulum Ca2(+)-ATPase activity in muscle homogenates, Anal. Biochem. 191 (1990) 321–331.
[23] A. Saborido, G. Moro, A. Megias, Transverse tubule Mg(2+)-ATPase of skeletal muscle. Evidence for extracellular orientation of the chicken and rabbit enzymes, J. Biol. Chem. 266 (1991) 23490–23498.
[24] J. Delgado, A. Saborido, M. Moran, A. Megias, Chronic and acute exercise do not alter Ca^{2+} regulatory systems and ectonucleotidase activities in rat heart, J. Appl. Physiol. 87 (1999) 152–160.
[25] J.L. Sapp, S.E. Howlett, Density of ryanodine receptors is increased in sarcoplasmic reticulum from prehypertrophic cardiomyopathic hamster heart, J. Mol. Cell. Cardiol. 26 (1994) 325–334.

[26] A. Saito, S. Seiler, S. Fleischer, Alterations in the morphology of rabbit skeletal muscle plasma membrane during membrane isolation, J. Ultrastruct. Res. 86 (1984) 277–293.
[27] R.D. Mitchell, P. Palade, A. Saito, S. Fleischer, Isolation of triads from skeletal muscle, Methods Enzymol. 157 (1988) 51–68.
[28] D.M. Bers, V.M. Stiffel, Ratio of ryanodine to dihydropyridine receptors in cardiac and skeletal muscle and implications for E–C coupling, Am. J. Physiol. 264 (1993) C1587–C1593.
[29] A. Margreth, E. Damiani, G. Tobaldin, Ratio of dihydropyridine to ryanodine receptors in mammalian and frog twitch muscles in relation to the mechanical hypothesis of excitation–contraction coupling, Biochem. Biophys. Res. Commun. 197 (1993) 1303–1311.
[30] S.U. Rajguru, G.S. Yeargans, N.W. Seidler, Exercise causes oxidative damage to rat skeletal muscle microsomes while increasing cellular sulfhydryls, Life Sci. 54 (1994) 149–157.
[31] A.M. Duke, D.S. Steele, Mechanisms of reduced SR Ca(2+) release induced by inorganic phosphate in rat skeletal muscle fibers, Am. J. Physiol., Cell Physiol. 281 (2001) C418–C429.
[32] H. Westerblad, D.G. Allen, The effects of intracellular injections of phosphate on intracellular calcium and force in single fibres of mouse skeletal muscle, Pflugers Arch. 431 (1996) 964–970.
[33] S. Matsushita, L. Dux, D. Pette, Separation of active and inactive (nonphosphorylating) Ca(2+)-ATPase in sarcoplasmic reticulum subfractions from low-frequency-stimulated rabbit muscle, FEBS Lett. 294 (1991) 203–206.
[34] M. Parreno, A. Pol, J. Cadefau, J. Parra, L. Alvarez, E. Membrilla, R. Cusso, Changes of skeletal muscle proteases activities during a chronic low-frequency stimulation period, Pflugers Arch. 442 (2001) 745–751.
[35] D.G. Allen, H. Westerblad, Role of phosphate and calcium stores in muscle fatigue, J. Physiol. 536 (2001) 657–665.